MULTI-SCALE IMAGING AND MODELING WORKFLOW TO CAPTURE AND CHARACTERIZE MICROPOROSITY IN SANDSTONE

Long H.[1], Nardi C.[1], Idowu N.[1], Carnerup A.[2], Øren P.E.[1], Knackstedt M.[2], Varslot T.[1], Sok R.M.[2]
Lithicon AS, Trondheim, Norway[1], and Canberra, Australia[2]

This paper was prepared for presentation at the International Symposium of the Society of Core Analysts held in Napa Valley, California, USA, 16-19 September, 2013

ABSTRACT

In this paper we describe an extensive imaging and modeling workflow which can be used to analyse not only conventional sandstone, but also tight gas sands. An important ingredient in this workflow is a difference mapping technique, which enables us to spatially characterize sub-resolution features using a pair of 3D tomographic images. By using the so-called dry/wet imaging sequence and combining two different micro computed tomography images of the same sample (one of the images is taken when the sample is in a dry and clean state while the other is taken when it is fully saturated with an X-ray attenuating fluid) we are able to compensate for insufficient image resolution in the estimation of porosity.

We present results for a sandstone sample which is rich in clay and where porosity estimates based on a single tomographic image was about 3% lower than what had been measured in the laboratory. Using the dry/wet technique we were able to match the laboratory measurements with only 0.1% difference.

We further apply a variation of the dry/wet technique to a tight gas sand where a significant fraction of the porosity is below the image resolution. In this case, we demonstrate the ability to match the micro-porosity to high-resolution mineralogical information to further characterize the sample.

The entire workflow is based on multiple integrated 2D SEM and 3D micro-CT image datasets, with the goal of characterizing various pore types and textures at different scales. Having developed an integrated model, detailing the different imaging and modeling techniques, we outline the upscaling of the petrophysical properties via a hybrid upscaling approach.

INTRODUCTION

To satisfy current energy demands, the oil and gas industry relies on being able to extract an increasing fraction of the available hydrocarbons from already-developed reservoirs,

as well as producing from the new so-called *unconventional sources; reservoirs typically in the micro-Darcy range*. In both cases great challenges remain, and a concerted technology effort is needed to improve the reservoir rock characterization from the nano-pore to the plug/core scale.

A reservoir characterization must include *in situ* porosities, saturations, and effective permeabilities. For conventional reservoirs, detailed information about the pore-scale geometry and connectivity is essential in order to understand the flow and trapping mechanisms, and thereby device a suitable recovery strategy [1, 11, 12, 17]. Tight oil and gas reservoirs further exhibit storage and flow characteristics that are intimately tied to depositional and diagenetic processes. As a result, exploitation of these resources requires a comprehensive multi-scale reservoir description and characterization program to identify properties which control production [4, 6].

Digital Rock Analysis (DRA) is currently emerging as a technology which can provide the data required to perform reservoir characterization and simulations; and thereby lead to an improved recovery factor in these challenging production regimes.

An essential step in DRA is to build a digital model. This model should display the same properties as the rock sample in question. One such property is porosity. In sandstones, porosity can be considered to occur as:

- primary intergranular porosity between detrital grains
- secondary porosity located in partially dissolved minerals (*e.g.*, feldspars and mica)
- microporous detrital grains and matrix (*e.g.*, microporous chert, glauconite, mud pellets)
- diagenetic minerals such as clay minerals (*e.g.*, chlorite, kaolinite, smectite, illite, etc.) and with varying distribution and growth habit (*e.g.*, pore filling, pore lining, pore bridging)

Total porosity alone, however, is not sufficient to accurately predict the rock quality, especially in tight gas sands with significant diagenesis [13]. Differentiation and quantification of the various porosity types, their connectivity in three dimensions (3D) and their contribution to overall porosity and flow, is an essential step in understanding and predicting the producibility of tight gas reservoirs. A multi-scale 3D approach to the characterization of the porosity, pore and throat size distribution, pore connectivity, permeability and petrophysical response is required to better characterize tight gas reservoir core. This should include characterizing the heterogeneity and connectivity of the key constituents (*e.g.*, porosity, cements, clays, porous minerals) at the nanometer, micron and millimeter scale, and imaging and analyzing the porosity, pore throats and connectivity at the nanoscale of these different constituent phases.

Integrated multi-scale imaging and modeling methods have been successfully applied in determining petrophysical and multiphase flow properties of reservoir rocks at the pore, micro-plug, plug and whole core scale for conventional reservoir core material [10, 11]. The method is based on the integration of multi-scale X-ray micro-CT imaging and numerical 3D rock modeling to characterize heterogeneity, pore classes and porosity types at different scales for the rock types identified in the samples. Petrophysical and multiphase flow properties are then calculated on the pore-scale and then upscaled to core plug and even whole core scales using a multi-stage upscaling technique. Case studies undertaken on conventional clastic and carbonate reservoirs have led to favorable comparisons with experimental conventional core analysis (CCA) and special core analysis laboratory (SCAL) predictions [10, 11].

In this paper we describe an extensive imaging and modeling workflow which can be used to analyse not only conventional sandstone, but also tight gas sands. Extending the workflow to tight gas sands includes the use of 2D and 3D image data obtained at multiple scales using micro-CT, 2D SEM, automated 2D SEM-EDS (quantified mineralogy) and 3D focused ion beam SEM (FIBSEM). The method is based on integrating these 2D and 3D image datasets, with the goal of characterizing various pore types and textures at different scales. This information is used to inform a calibrated multiscale integration of the petrophysical properties of the rock sample. We first describe the development of the integrated model, detailing the different imaging and modeling techniques (with examples) and secondly outline the upscaling of the petrophysical properties via a hybrid upscaling approach.

MULTI-SCALE IMAGING AND ANALYSIS WORKFLOW

A brute-force calculation of properties which account for both clay microstructure (10-100 nm) yet span the scale of a tight sand plug (40 mm) is not realistic with current computational resources. Instead, we integrate the information collected at different scales using a continuum network approach. To this end, a five-stage multi-scale analysis workflow is used and described below:

1. 3D micro-CT images are acquired at different resolutions and internally registered to generate a primary grain structure representation of the core material. Microporosity and mineralogy is mapped via difference imaging mapping methods and correlation to SEM/SEM-EDS analysis at similar resolutions.
2. Higher-resolution SEM and FIBSEM images characterize the 2D and 3D structures required to describe the geometry and topology for the pore filling and microporous pore structures.
3. Modelling of clay/microporous volumes is required to give input for flow data in the continuum network. Using the 3D structural information of the microporous phases identified via SEM/SEM-EDS and FIBSEM, we generate a range of models associated with variable clay microstructures/depositional and diagenetic

history. These microstructures are all correlated to FIBSEM image data. Properties are calculated for the models of the small microstructures.

4 The microporosity map generated in (1) is the base of assigning properties for the sub-resolution pores structures in an upscaling routine.

5 Petrophysical and multiphase flow properties are then computed for each key phase and up-scaled to the plug scale using upscaling procedures based on appropriate use of volume averaging and Darcy's law.

IMAGING AT MULTIPLE SCALES

Plug scale micro-CT imaging

Plug scale images are obtained via micro-CT imaging on 1 or 1 ½ inch plugs at resolutions of 10 or 20 micron/voxel; rock type variations, zones of cementation, laminations at the resolution can be characterized. Using the *Heliscan* technique we can image plugs of length 100 mm in aspect ratios of 5:1 [15].

Pore scale Micro-CT imaging

Micro-CT imaging is undertaken at the pore scale on sandstone sub-samples, *i.e.*, micro-plugs with diameters of 3-10 mm drilled from the corresponding core plugs. The resolution of the images is a factor of 2000x smaller than the sample diameter (*e.g.*, 4 mm diameter has ~2 micron resolution, 10 mm diameter ~5 micron resolution). Imaging is first undertaken under *as received* conditions. In order to accurately quantify sub-resolution porosity, the difference mapping approach using a dry/wet experiment is performed, as described extensively in the following section.

Difference image mapping for porosity estimation and sub-resolution phase mapping

The general workflow of *difference image mapping* is applied to two tomograms of the same sample at two different experimental states. The three main stages of the workflow are (1) registration, (2) intensity scaling and (3) pointwise intensity subtraction. The accurate registration [8] and appropriate scaling of the intensities are necessary so that in the differencing step the regions of the sample that have not changed in the experiment cancel out. This general workflow can be applied multiple times to monitor the change at different stages during an experimental sequence. Spatial mapping of various quantities, such as oil and gas saturation, can similarly be quantified using analogous difference imaging schemes. Depending on the sample, a number of micro-CT images with varying contrast agents and at various saturation states may therefore be acquired. For heterogeneous samples, one set of images is acquired for a micro-plug from each major rock type.

As an example, we show the simple case of dry/wet difference mapping where we take the difference between an image of a sample in a cleaned and dry state and an image of the same sample fully saturated with an X-ray attenuating fluid. The advantage of this approach as compared to inferring the pore space from a single tomogram becomes

evident once one investigates samples with different attenuating minerals and/or sub-resolution porosity (micro-porosity). In the dry/wet difference mapping, a difference will only be visible where the attenuating fluid has entered the sample. As long as we use X-rays in an energy band well above the relevant K-edges, and as long as care is taken to avoid significant beam-hardening effects, the difference will be proportional to the amount of fluid which has entered the volume covered by each voxel, irrespective of sample composition or imaging resolution.

Example

In the oil and gas industry, reservoir rock with high quartz gain, and low feldspar and matrix content is defined as conventional sandstone, which has high porosity (12 to 30%) and high permeability (> 0.1 mD) [16]. A 6 mm diameter micro-plug was extracted from a conventional open sandstone plug, and imaged in a clean, dry state using an X-ray micro-CT at a resolution of 3.5 µm/voxel. A slice of the dry tomogram, along with a segmentation into the phases: open porosity, micro-porosity and solid minerals is given in Fig. 1. A porosity profile, also included in Fig. 1, indicates that the sample is very homogeneous. It is therefore natural to expect the porosity in the imaged micro-plug to closely match that of the sister plug used to obtain lab-based porosity measurements. In this case, the laboratory measurements (MICP) showed a porosity of 21.7%

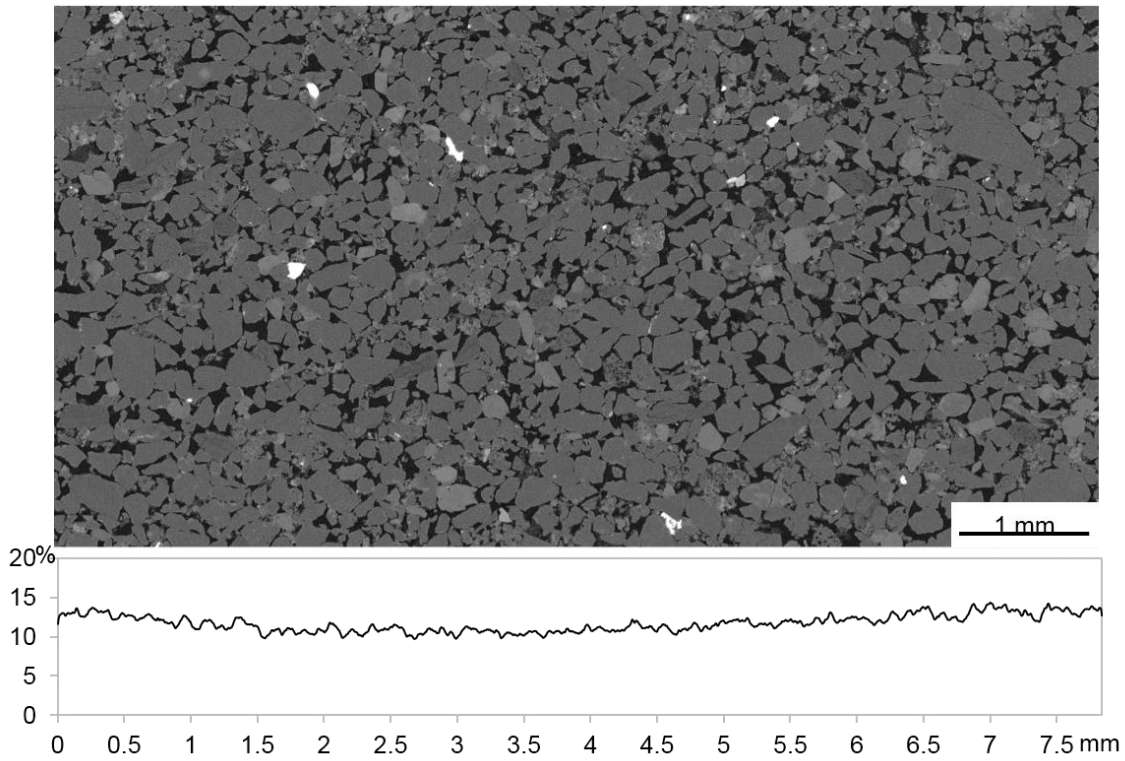

Fig. 1: Top panel displays a cross-section from the tomogram of the sample in its clean and dry state. The bottom panel shows a porosity profile of this tomogram; the open (resolved) porosity estimated for each slice perpendicular to the height-axis of the micro-plug.

To demonstrate the importance of the dry/wet difference mapping in obtaining a good segmentation, we compare three different scenarios: (1) segmentation from dry tomogram using a converging active contours (CAC) algorithm, (2) forced porosity matching and (3) dry/wet difference mapping.

First we perform a set of CAC segmentations [14] to identify the different minerals with sub-resolution porosity as well as those that can be defined from the dry tomogram alone. We then assign an average porosity of 30% (which was previously determined by careful comparison to different sub-resolution porous phases) to the microporosity phase and estimate the total porosity. This approach relies on the assumption that the micro-porous regions can be accurately determined from the X-ray attenuation. This is a flawed assumption in particular in the presence of strongly attenuating clay material. In our case, the total porosity using this approach comes in on 18.3%. This is 3.4 p.u. below the experimental porosity, and is too low, as can be verified by comparing it to an intersecting high-resolution SEM slice.

A second scenario focuses on correctly matching the experimental porosity (forced porosity matching). Since porosity is such a fundamental property, this is a tempting approach. It is generally achieved by choosing an appropriate segmentation threshold to match the measured porosity. This approach is also flawed, as it results in a poor representation of the pore space of the rock (see Fig. 2). The sandstone under investigation contains many microporous mineral phases with different X-ray attenuations, amongst which a significant fraction of iron-rich clays including chlorite. The porosity can therefore not be identified based solely on the X-ray attenuation of the dry core material.

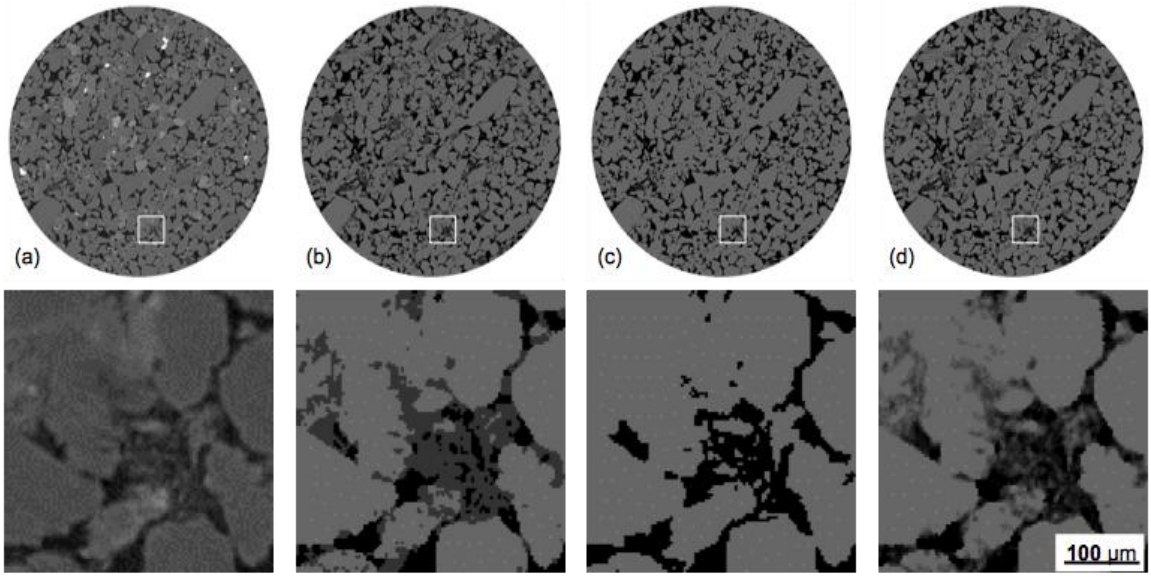

Fig. 2: Comparison of the various segmentations for a conventional sandstone tomogram. (a) tomographic image, (b) dry-only CAC segmentation, (c) forced-porosity segmentation, and (d) segmentation based on the difference mapping technique.

The third scenario comprises of the use of the dry/wet difference mapping segmentation explained above. The final porosity from this segmentation comes to 21.8%. The close match of the experimental porosity is rather fortuitous, but experience shows that for homogeneous samples like this, it is generally possible to achieve agreement within 1 p.u.

The implications of the poor representation of pore space in the forced-porosity approach can be clearly demonstrated by investigating the pore space further and comparing the resultant simulated permeabilities (Lattice-Boltzmann). The main geometric feature which is important for the permeability is the critical diameter, which is defined as the diameter of the largest sphere which can pass through the system. Figure 3 compares the distribution of this critical diameter computed for sub-sets of the dry/wet difference mapping to that of the forced porosity matching method. Note that the total porosity in both segmentations are almost identical. The median critical diameter of the forced porosity matching segmentation turns out to be significantly larger (22%) than that of the dry/wet mapping. The resulting permeabilities show this effect even clearer; k=1400mD for the forced porosity segmentation vs. k=570 mD for the dry/wet difference mapping segmentation, almost 2.5 x larger. The experimental permeability for the plug is ~450 mD.

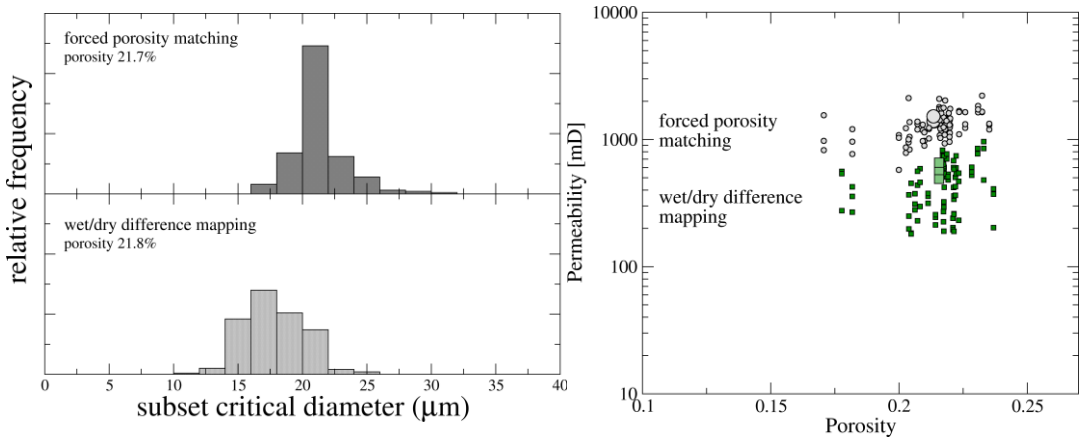

Fig. 3: Distribution of critical diameter (left) and permeability (right) computed for subsets of the segmentation with forced porosity matching, and for segmentation based on dry/wet difference mapping.

Micro-porosity and mineral mapping with SEM

To characterize the sub-resolution porosity, the micro-plug is cut and a face within the 3D field of view is exposed. This face is polished for the acquisition of scanning electron microscopy (SEM) images. The SEM images are registered into the 3D volume using image registration software [8]. This enables a pixel-by-pixel comparison between high-resolution SEM and the corresponding slice from the micro-CT data. In Fig. 4 we see the microporous region identified in the dry/wet difference map overlaid on top of a high-resolution SEM image. Clearly, this allows quality control of the segmentation. More

importantly, however, this allows the porosity map to be calibrated using estimates obtained at a much higher resolution.

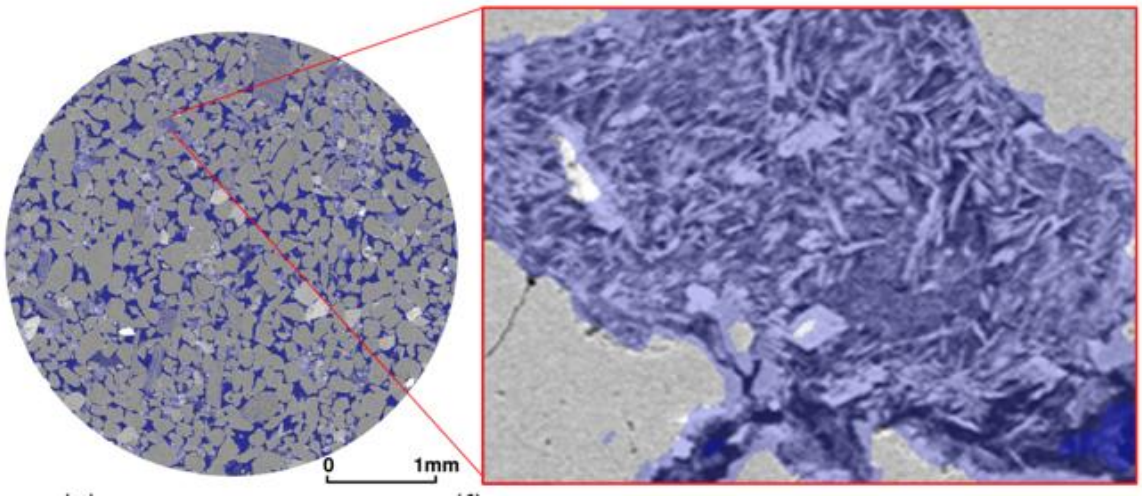

Fig.4: SEM image of the conventional sandstone overlaid with the identified micro-porosity from the dry/wet difference map. Combining high-resolution 2D imagery with the 3D tomographic image enables quality control of the segmentation, as well as further investigation and characterization of the micro-porous structure at varying resolutions.

Automated mineral identification of the same face can also be obtained using energy-dispersive SEM (QEMScan / EDS-SEM), thereby correlating the tomographic information also mineralogy information. Figure 5 shows how the micro-porous regions of a tight gas sand with a range of open to closed kaolinite. The 4mm sample (permeability ~0.1 mD, resolution 2.5 micron) was imaged by dry/wet difference mapping, cut, polished and imaged by SEM and EDS-SEM.

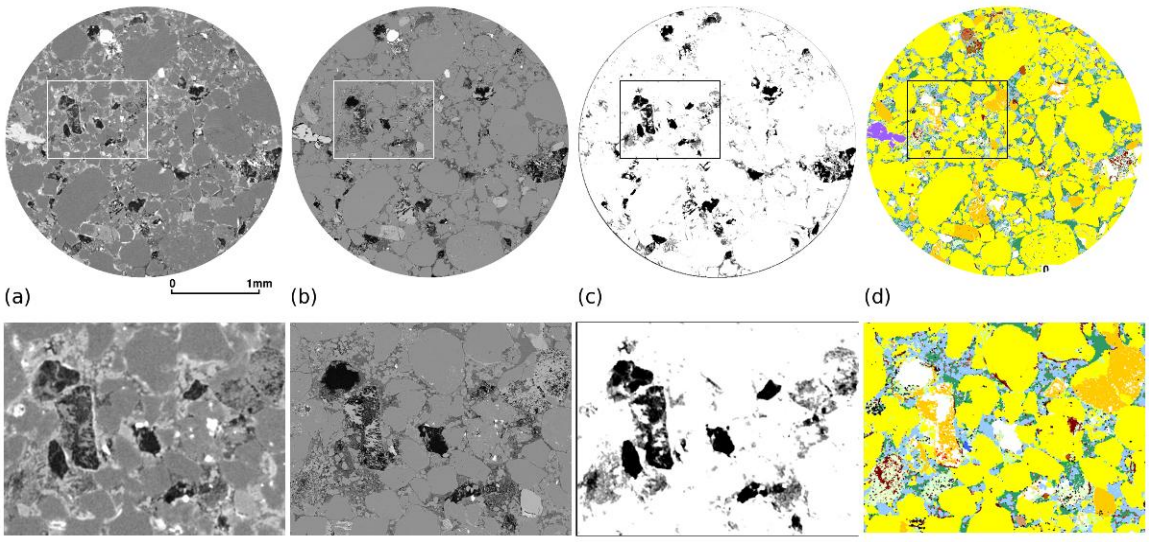

Fig. 5: Tight gas sample exhibiting a range of open to more closed kaolinite. (a) Dry tomogram at 2.5 micron resolution. (b) Registered SEM (c) Porosity map from wet/dry difference (d) Registered automated

mineralogy mapping through EDS-SEM, the main phases are open porosity (white), quartz (yellow) and kaolinite (green). .

Coupling of image data from SEM/SEM-EDS with the micro-CT image block thus enables one not only to quality control the identification of the constituent phases in 3D. It also enables one to characterize various pore types (disconnected, porosity above a pore scale cutoff, clay bound versus effective, *etc.*) and textures in 3D as well as providing a calibrated estimate of the overall plug porosity.

Characterizing nano-scale features via FIBSEM imaging

For tight samples, where regions identified as microporous need to be characterized at nanometric scales, we apply a critical selection method to identify regions of interest for higher-resolution investigation. Nanoporous 3D imaging via FIBSEM can then be undertaken on important microporous features which are deemed critical to the petrophysical and flow response of each sample.

MODEL DEVELOPMENT

Building nanoscale pore structures

From the key 3D nanoporous features (*e.g.*, structures and distributions of important diagenetic clay microstructures) we can develop appropriate representations of these nano-porous models, and derive drainage capillary pressure and relative permeability curves, which can be applied back into the pore and plug scale models, Fig. 6 [10, 11].

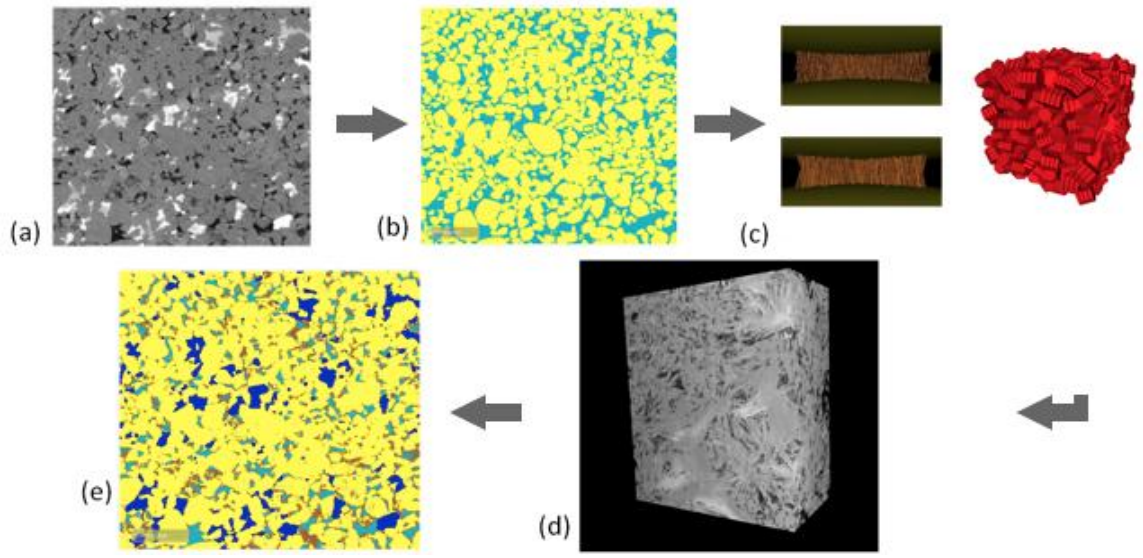

Fig. 6: (a) 3D tomographic data are used to seed the (b) original grain structure. (c-d) Higher resolution descriptions of pore filling and inter/intragranular pore filling/lining/blocking material are used to decorate the grain structure to give (e) a more realistic multi-scale description of the pore structure of the tight reservoir sand.

Upscaling of the petrophysical properties via a hybrid upscaling approach

Petrophysical and multiphase flow properties are computed for each key phase and up-scaled to the plug scale using upscaling procedures based on volume averaging and Darcy's law, the details of which will be discussed in a future publication. Figure 7 (a-c) show the intergranular, microporous and complete pore scale description of the sample shown in figure 5.

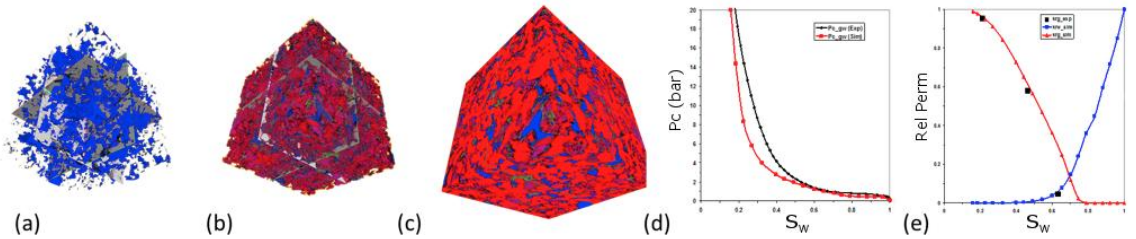

Fig. 7: (a) Image of the 3D distribution of the intergranular pore space, (b) the intergranular (blue) + microporous (dark red) and (c) the whole rock (grains in bright red and green). d-e show the resultant drainage capillary pressure and relative permeability curves from the model prediction compared with experiment (black curves and data points).

From the multiscale digital rock description we can derive petrophysical properties such as permeabilityand formation factor (finite element) directly on the sample. Transport properties, such as relative permeability and capillary pressure, are determined from multiphase flow simulations using network simulators (see Fig. 7 (d-e)).

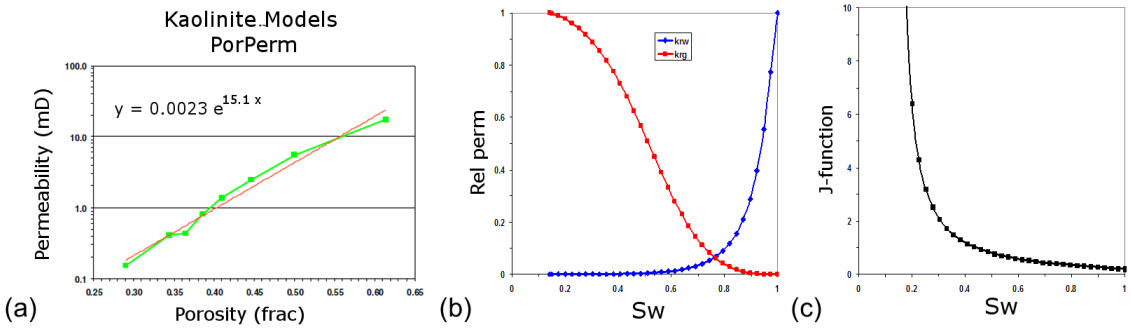

Fig 8: (a) Porosity:permeability trend for kaolinite derived from nanoporous structural models. (b,c) Drainage capillary pressure and relative permeability curves derived at one particular porosity value for the nanoporous model.

Further Quality Control

A final anchoring study can be based on *pore* scale comparison of the predictions of multiphase flow simulations to endpoint experimental data from imaging. 3D imaging of endpoint fluid distributions at residual conditions enables one to undertake an anchoring and calibration of pore network based modelling methods on the same core material and

will help in calibrating the PNM methods for multiphase flow. A case study of this has been undertaken by (Bhattad *et al.*, 2013) and is presented separately in the Proceedings.

CONCLUSIONS

It has been shown that the accuracy of porosities estimated from segmented micro-CT images are fundamentally limited by the tomographic image resolution in conventional sandstones as well as in tight gas sands where a significant fraction of the porosity is below the image resolution. To compensate for the insufficient image resolution, a difference mapping technique is presented in this paper.

The use of dry/wet difference mapping leads to a better characterization of the pore space. This technique allow us to define the sub-resolution porosity which is of importance while computing petrophysical properties for instance. Comparison of three different methods of obtaining porosity from micro-CT images shows clearly that the converging active contours method results in lower porosity estimate while forcing the porosity to match experimental data. However, the implications of the poor representation of pore space in the forced-porosity approach can be clearly demonstrated by investigating the pore space further and comparing the resultant simulated permeabilities (lattice-Boltzmann). The pore space obtained by forcing segmentation approach result in a large deviation in the absolute permeability. Whereas, porosity and permeability derived from the dry/wet difference mapping technique are very comparable with the experimental data. Dry/wet difference mapping shows also how the micro-porous regions of a tight gas sand with a range of open to closed kaolinite to capture the microporosity in the unconventional sandstone.

In terms of multi-phase flow, multi-scale digital rock descriptions that incorporate information from the different phases are required as inputs by the network simulators. Prediction of macroscopic transport properties such as capillary pressure and relative permeability on the digital rock can then be done using upscaling procedures that are based on volume averaging and Darcy's law.

ACKNOWLEDGMENTS

The authors acknowledge Lithicon (Norway and Australia) for granting permission to publish this paper which is partly funded by RWE Dea and Norwegian Research Council through PETROMAKS Project Number: 208772/E30, titled: "Physically based three-phase relative permeability relations". We also thank STATOIL and TOTAL, for their contribution.

REFERENCES

[1] Bakke, S., and Øren, P. L. E., *3-D pore-scale modelling of sandstones and flow simulations in the pore networks*, SPE Journal, *2*(2), 136-149, (1997).

[2] Fogden, A & Lebedeva, E., *Changes in wettability state due to waterflooding*, in Proc. of Society of Core Analysts, SCA-2011-15, (2011).
[3] Golab, A, Knackstedt, M, Averdunk, H, Senden, T, Butcher, A & Jaime, P., *3D Porosity and mineralogy characterization in tight gas sandstones*, The Leading Edge, December, pp. 936-942, (2010).
[4] Kamath, J. and Boyer, R.E., *Critical gas saturation and supersaturation in low-permeability rocks*, SPE Formation Evaluation, (1995).
[5] Kalam, Z, Seraj ,S, Bhatti, Z, Mock, A, Lopez, O., Mock, A., Ravio, R, Øren, P.E., *Relative permeability assessment in a giant carbonate reservoir using Digital Rock Physics*, in Proc. of Society of Core Analysts, SCA2012-03, (2012).
[6] Klimentidis, R. and Welton, J.E., *Advances in reservoir quality assessment of tight-gas sands - Links to producibility*, AAPG Annual Convention, San Antonio, Texas, April 20-23, 2008, (2009).
[7] Knackstedt, M.A., Senden, T.J., Carnerup, A., Fogden, A., *Improved characterization of EOR processes in 3D. Characterizing mineralogy, wettability and residual fluid phases at the pore scale*, SPE Enhanced Oil Recovery Conference, Kuala Lumpur, Malaysia, July, SPE 145093, (2011).
[8] Latham, S., Varslot, T., and Sheppard, A., *Image registration: Enhancing and calibrating X-ray micro-CT imaging*, in Proc. *Society of Core Analysts*, Abu Dhabi, UAE, SCA2008-35, (2008).
[9] Lebedeva, E.V., Fogden, A., *Micro-CT and wettability analysis of oil recovery from sand packs and the effect of waterflood salinity and kaolinite*, Energy & Fuels 25, 5683-5694, (2011).
[10] Lopez, O., Mock, A., Oren, P.E., Long, H., Kalam, Z., Vahrenkamp, V, Gibrata, M., Seraj, S., Chacko, S, Al Hammadi, M., Al Hosni, H., Sahn, H., Vizamora, A., *Validation of fundamental carbonate reservoir core properties using Digital Rock Physics*, in Proc. of Society of Core Analysts, SCA2012-19, (2012).
[11] Lopez, O., Mock, A., Skretting, J., Peteresen, E.B, Oren, P.E., Rustad, A. B., *Investigation into the reliability of predictive pore scale modelling in siliclastic reservoir rocks*, in Proc. of Society of Core Analysts, SCA2010-23, (2010).
[12] Nardi, C., Lopez, O., Øren, P. E., Held, R., and Petersen Jr, E. B., *Pore-Scale Modeling of Three-Phase Flow: Comparative Study with Experimental Reservoir Data*, in proceeding of Society of Core Analysts, SCA2009-30, (2009).
[13] Rushing, J.A., Newsham, K.E. and Blasingame, T.A., *Rock typing – Keys to understanding productivity in tight gas sands*, SPE paper 114164, (2008).
[14] Sheppard, A.P., Sok, R.M. and Averdunk, H.,*Techniques for image enhancement and segmentation of tomographic images of porous materials*, Physica A, 229(1-2), (2004).
[15] Varslot, T., Kingston, A., Myers, G., and Sheppard, A.P., *High-resolution helical cone-beam micro-CT with theoretically-exact reconstruction from experimental data*, Medical Physics, 38(10), (2011).
[16] Zou, C., *Unconventional Petroleum Geology*, Newnes, (2012), 68.

[17] Øren, P. E., & Bakke, S., *Reconstruction of Berea sandstone and pore-scale modelling of wettability effects*, Journal of Petroleum Science and Engineering, 39(3), 177-199, (2003).